

HIGH-RESOLUTION INVESTIGATION OF THE REACTION $^{35}\text{Cl}(p, \alpha_0)^{32}\text{S}$

B. BOŠNJAKOVIĆ, J. BOUWMEESTER, J. A. VAN BEST and H. S. PRUYS

Fysisch Laboratorium der Rijksuniversiteit, Utrecht

Received 19 December 1967

Abstract: The $^{35}\text{Cl}(p, \alpha_0)^{32}\text{S}$ reaction is investigated in the energy region $E_p = 830\text{--}2\,930$ keV; 76 resonances are observed. Resonance energies, strengths and widths are reported. The analysis of α_0 angular distributions, measured at 58 resonances, allows unique spin and parity assignments in 24 cases. In most other cases, two or three $J\pi$ assignments remain possible. Formation and population parameters are determined. Resonances showing significant f-wave proton capture are discussed as possible isobaric analogues of corresponding states in ^{36}Cl .

E

NUCLEAR REACTION $^{35}\text{Cl}(p, \alpha_0)$, $E = 0.83\text{--}2.93$ MeV; measured $\sigma(E_p; \theta)$.
 ^{36}Ar deduced levels, strengths, J, π , formation and population parameters.
Enriched target.

1. Introduction

Resonance states of ^{36}Ar have been investigated through the $^{32}\text{S}(\alpha, \gamma)^{36}\text{Ar}$ and the $^{35}\text{Cl}(p, \gamma)^{36}\text{Ar}$ reactions by Ern  *et al.*¹⁻³⁾. They were also studied with lower energy resolution in the reaction $^{35}\text{Cl}(p, \alpha_0)^{32}\text{S}$ by Clarke *et al.*⁴⁾ and by Karad ev *et al.*⁵⁾. In the experiment of Kuperus *et al.*⁶⁾, no α -particles resulting from the latter reaction were observed in the $E_p = 200\text{--}850$ keV region.

The investigation of resonance reactions in the s-d shell region has achieved new significance through the concept of isobaric spin. A study of the $^{37}\text{Cl}(p, \alpha_0)^{34}\text{S}$ reaction^{7,8)} revealed several attractive properties of the (p, α) reaction as a tool for obtaining information on isobaric analogue states. It was felt, therefore, that the $^{35}\text{Cl}(p, \alpha_0)^{32}\text{S}$ reaction should be studied in a systematic way with improved energy resolution. The present investigation indicates that also in the case of the ^{36}Ar nucleus, the (p, α) reaction can be used for identification of isobaric analogue states.

2. Experimental techniques

Protons were accelerated up to 3 MeV with the Utrecht Van de Graaff generator and bombarded targets of BaCl_2 enriched in ^{35}Cl to 99.5%. Targets with thicknesses varying from 5 up to 50 $\mu\text{g}/\text{cm}^2$, were prepared by evaporation of the target material onto thin carbon foils[†]. Mechanically, formvar backings are much less fragile than

[†] The carbon foils, which were 5 and 10 $\mu\text{g}/\text{cm}^2$ thick (type S5 and S10, respectively) were obtained from the Yissum Research Development Company, Jerusalem.

carbon backings, but they have to be discarded because of fast deterioration under proton bombardment. A 1 MeV proton beam of more than $0.1 \mu\text{A}$ destroys a formvar backing immediately, whereas carbon foils of the same thickness can easily stand a proton beam of up to $1 \mu\text{A}$.

Charged particles were detected with semi-conductor detectors placed at lab angles of 172° , 150° , 135° , 120° , 105° , 87° and 72° with respect to the beam. The experimental set-up has been described more extensively in ref. ⁸).

The low Q -value of the $^{35}\text{Cl}(p, \alpha_0)^{32}\text{S}$ reaction ($Q = 1.865 \text{ MeV}$) requires special care for reduction of proton pile-up. Whereas in the $^{37}\text{Cl}(p, \alpha_0)^{34}\text{S}$ reaction ($Q = 3.030 \text{ MeV}$) the background is mainly caused by higher-order pile-up, the α_0 group from the proton bombardment of ^{35}Cl is obscured by the stronger second-order

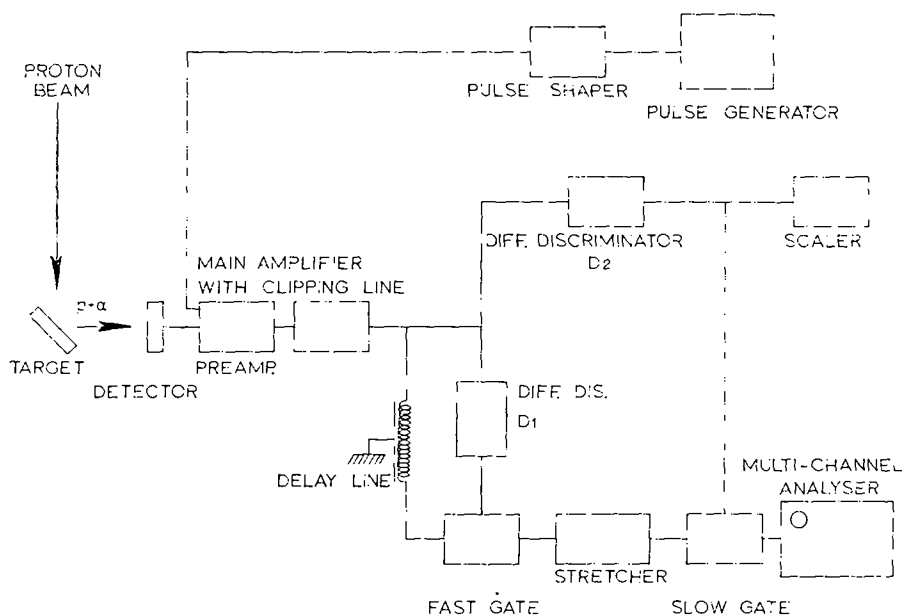


Fig. 1. Block scheme of the electronics for one detector; details are described in the text.

pile-up. The low background in the excitation curve (see sect. 3) was obtained mainly by (i) use of several detectors with small solid angles instead of one detector with a large solid angle and (ii) narrow setting of the α_0 channels. In order to fulfill the latter requirement, slight changes in the electronics were necessary. The block scheme is given in fig. 1. The output of the pre-amplifier is fed to the main amplifier with 80 ns delay clipping. The short clipping time effectively cuts down the proton pile-up. The output of the main amplifier can be analysed with differential discriminator D2 and/or with a multi-channel analyser. To be accepted by the analyser, the clipped pulses have to pass a pulse lengthener which increases the pile-up in the analyser. To prevent this, a fast gate triggered by the discriminator D1 is used. Partly, the pile-up background

is suppressed by the dead-time of the discriminator. Moreover, the lower level of D1 can be set so that pile-up generating pulses may not pass the fast gate. The overall effect is that the pile-up will be low in the analyser too, thus making possible narrow

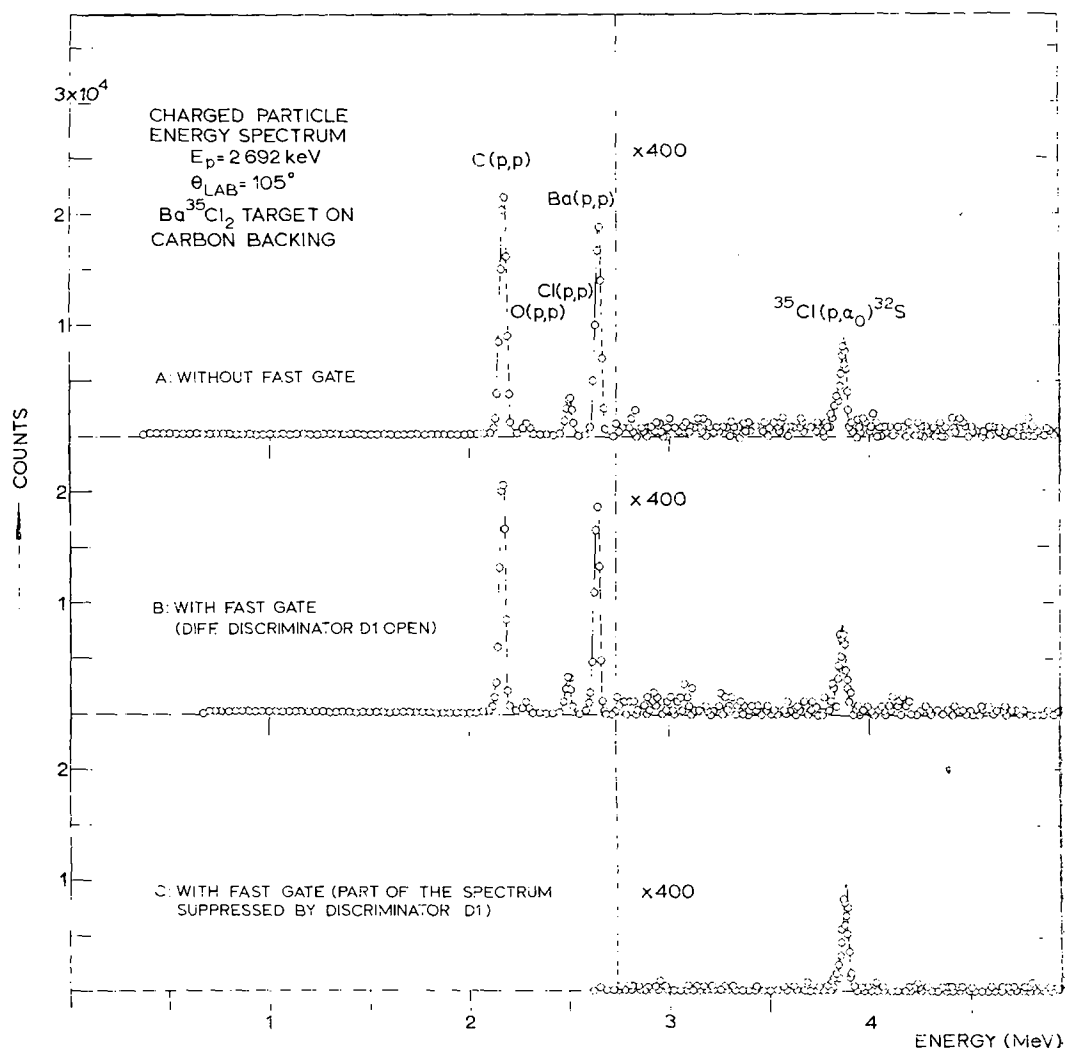
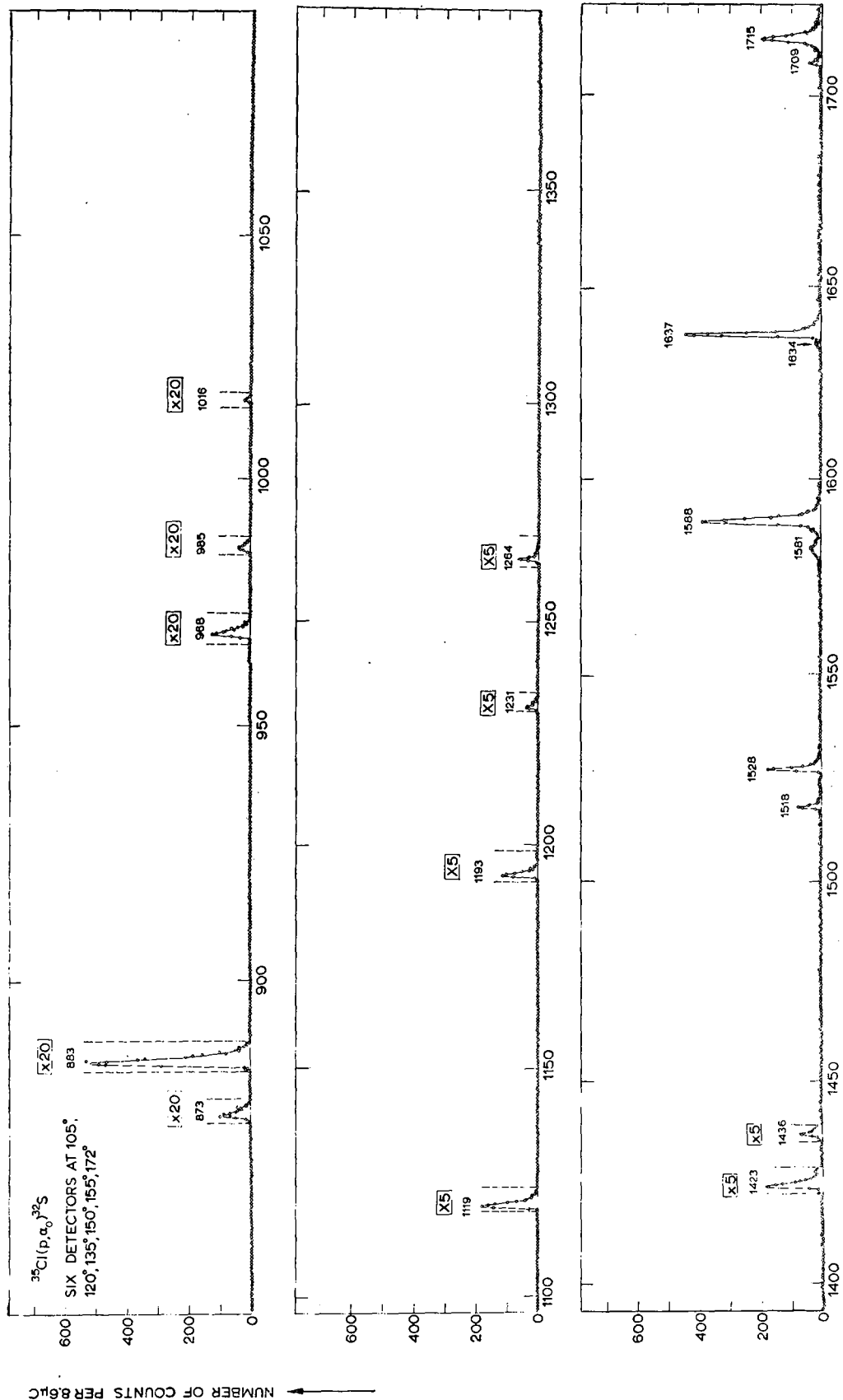


Fig. 2. Pile-up suppression, demonstrated in the particle energy spectrum at the $E_p = 2692 \text{ keV}$ resonance. A. Without the use of the fast gate, the heavy pile-up background is clearly seen. B. Pile-up is partly suppressed by the dead time of the discriminator D1. C. Pile-up is even more suppressed after the elastic scattering peaks are cut off.

setting of the α_0 channel even at weak resonances. Combinations of the described set-up with a low proton current of about 150 nA made feasible the detection of resonances with strengths down to several eV.



→ PROTON ENERGY (keV)

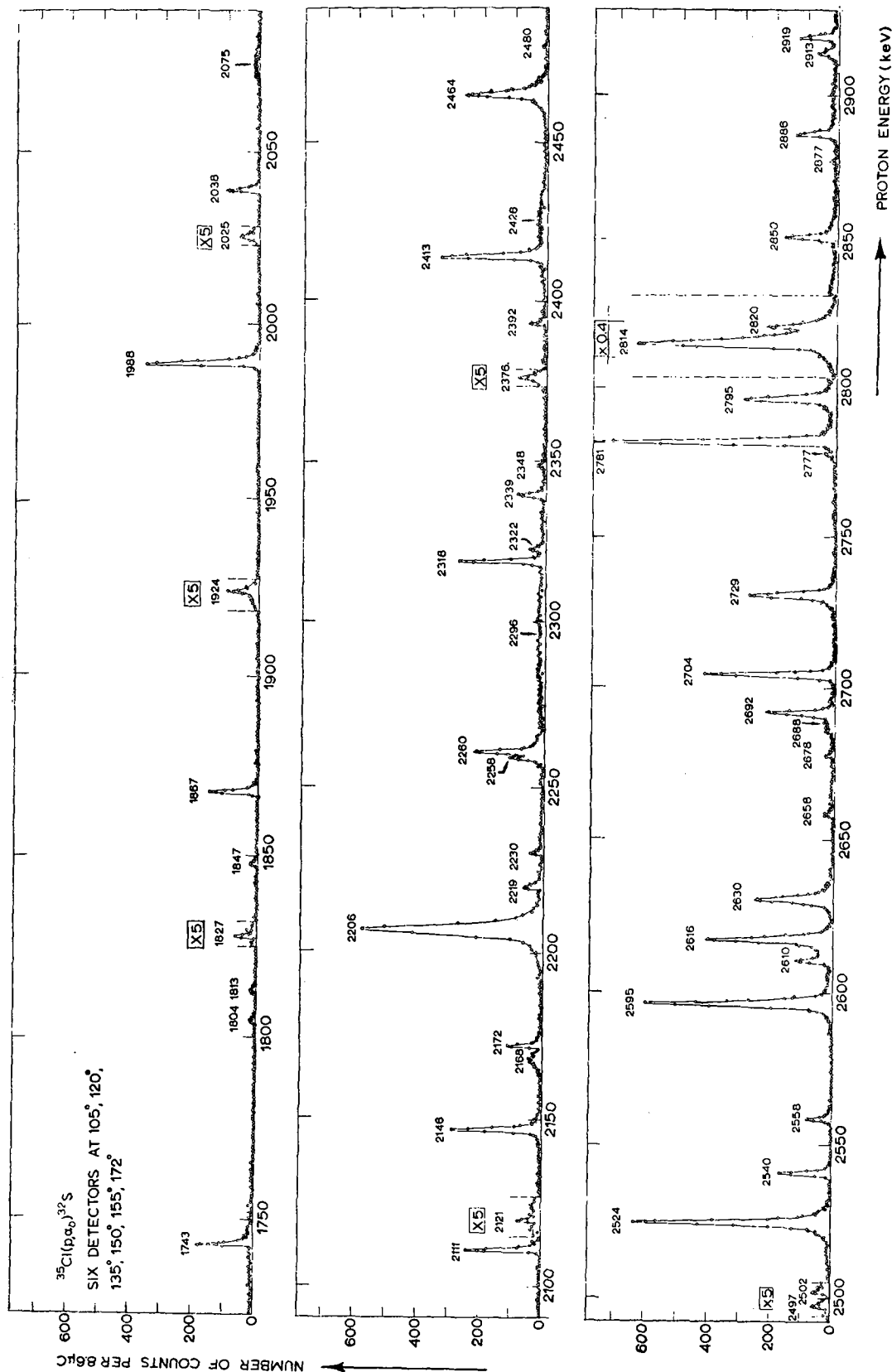


Fig. 3. Alpha-particle yield curve for the reaction $^{35}\text{Cl}(p, \alpha_0)^{32}\text{S}$. The thickness of the target is $5 \mu\text{g}/\text{cm}^2$.

A typical charged-particle spectrum is shown in fig. 2A. The α_0 group emitted from the compound state of ^{36}Ar to the ground state of ^{32}S appears as a peak at $E_\alpha = 3.88$ MeV. The α -particles populating higher ^{32}S states are completely obscured by scattered protons. The groups of elastically scattered protons, seen at lower energies, can be assigned to scattering on carbon, contaminant oxygen, chlorine and barium. These intense proton groups cause an appreciable second- and higher-order pile-up background, which is also partly shown. In figs. 2B and C, the suppression of the pile-up background is demonstrated.

3. The excitation curve

The yield of the α_0 particles from the $^{35}\text{Cl}(p, \alpha)^{32}\text{S}$ reaction was measured as a function of the proton energy with five detectors at angles between 105° and 172° .

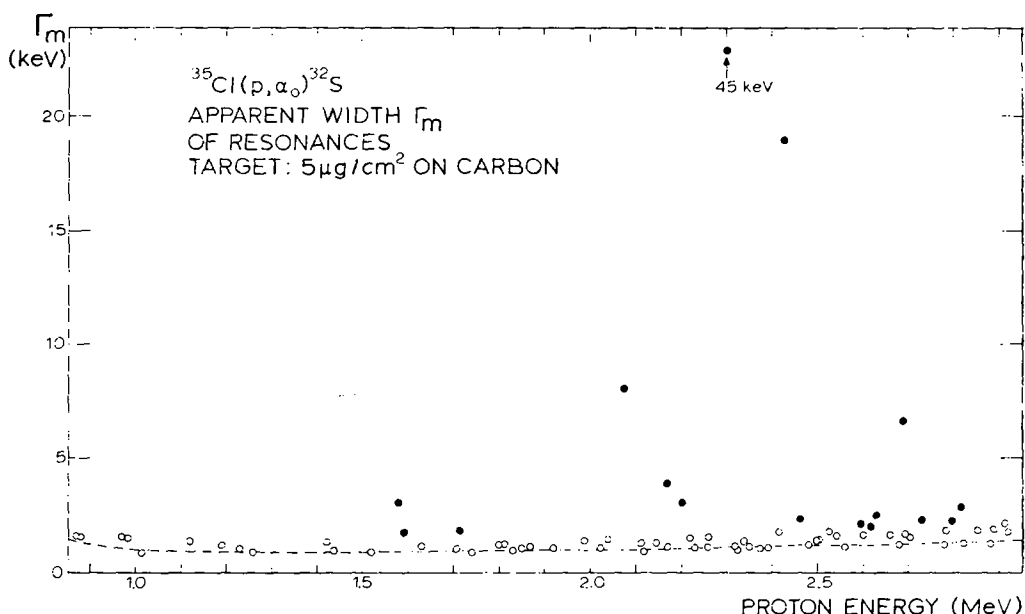


Fig. 4. Apparent width Γ_m of resonances plotted as a function of the proton energy in the 0.9-2.9 MeV region. Target thickness is $5 \mu\text{g}/\text{cm}^2$. The dashed curve is interpreted as the instrumental width Γ_i . The circles represent the "narrow" resonances, the dots correspond to resonances with a measurable natural width. The dashed curve is interpreted as the instrumental width.

The yield curve for proton energies between $E_p = 830$ and 2930 keV is given in fig. 3. The target thickness corresponds to an over-all energy spread varying from 0.9 to 1.4 keV. The excitation curve was measured in steps of maximally 0.6 - 1.0 keV, depending on E_p .

At several strong resonances, the yield of the $^{35}\text{Cl}(p, \gamma)^{36}\text{Ar}$ reaction was measured simultaneously with a $10 \text{ cm} \times 10 \text{ cm}$ NaI(Tl) scintillation crystal, positioned at 135° to the beam. The γ -ray yield curve is known from measurements by Ern  and Endt ²).

TABLE I
Resonances in the reaction $^{35}\text{Cl}(p, \alpha_0)^{32}\text{S}$;
energies, strengths, widths, competing gamma decay and J^π values

E_p (keV)	$E_x(^{36}\text{Ar})$ (keV)	$(2J+1)I_p I_{\alpha_0}/I'$ (eV)		I' (keV)	Gamma decay	J^π	
		this work	ref. ^{b)}			this work	other work ^{c)}
873.2 \pm 1.1	9 355	1.2		< 0.5	(γ^a)	1 ⁻ , 2 ⁺	2 ⁺ ^{c)}
883.4 \pm 1.1	9 365	8		< 0.5	(γ^a, b)	1 ⁻	
968.0 \pm 1.2	9 447	1.8		< 0.5	(γ^a)	1 ⁻ , 2 ⁺ , 3 ⁻	
985.5 \pm 1.2	9 464	0.5		< 0.5	(γ^a, b)	(0 ⁺), 1 ⁻ , 2 ⁺ ^{f)}	
1 015.8 \pm 1.2	9 494	0.19		< 0.5			
1 119.4 \pm 1.3	9 594	12		< 0.5	(γ^a, b)	1 ⁻ , 2 ⁺	2 ⁺ ^{d)}
1 192.6 \pm 1.3	9 666	7		< 0.5	(γ^a, b)	1 ⁻ , 3 ⁻	
1 230.7 \pm 1.4	9 703	2.0		< 0.5		0 ⁺ , 1 ⁻ , 2 ⁺	
1 264.0 \pm 1.4	9 735	3.1		< 0.5	(γ^a, b)	1 ⁻ , 3 ⁻ , 4 ⁺	
1 423.4 \pm 1.5	9 890	14		< 0.5	(γ^a, b)	1 ⁻ , 2 ⁺	
1 436.3 \pm 1.5	9 902	2.8		< 0.5	(γ^a, b)	4 ⁺ , (5 ⁻) ^{f)}	
1 518.1 \pm 1.6	9 982	22		< 0.5	(γ^a, b)	1 ⁻ , 3 ⁻	
1 527.7 \pm 1.6	9 991	60		< 0.5	(γ^a, b)	1 ⁻ , 2 ⁺	
1 581.5 \pm 2.0	10 044	24	410	2.1 \pm 0.5	(γ^a, b)	1 ⁻ , 2 ⁺	1 ⁻ , 2 ⁺
1 588.3 \pm 2.0	10 050	240		0.9 \pm 0.5	(γ^b)	3 ⁻	
1 634.3 \pm 2.0	10 095	6	210	< 0.5	(γ^a)		1 ⁻ , 3 ⁻
1 637.0 \pm 1.8	10 098	180		< 0.5	(γ^b)	1 ⁻ , 3 ⁻	
1 708.8 \pm 2.0	10 167	15	324	< 0.5	(γ^a, b)	1 ⁻ , 3 ⁻	1 ⁻ , (2 ⁺)
1 714.9 \pm 2.0	10 173	150		0.9 \pm 0.5	(γ^a, b)	1 ⁻ , 2 ⁺	
1 743.1 \pm 1.8	10 201	80	140	< 0.5			(1 ⁻), 2 ⁺
1 804.1 \pm 2.1	10 260	8		< 0.5			
1 812.6 \pm 2.1	10 268	13		< 0.5	(γ^a)	1 ⁻	
1 827.4 \pm 2.1	10 283	2.6		< 0.5			
1 847.3 \pm 1.9	10 302	13		< 0.5	(γ^a)	(4 ⁻) ^{g)}	4 ⁺ ^{d)}
1 867.1 \pm 1.9	10 321	80	320	< 0.5		2 ⁺	1 ⁻ , (2 ⁺)
1 923.6 \pm 2.1	10 376	6		< 0.5			
1 988.1 \pm 2.0	10 439	250	430	< 0.5		1 ⁻ , 2 ⁺	0 ⁺ , 2 ⁺
2 025.0 \pm 2.2	10 475	4.7	105	< 0.5		(3 ⁻), 4 ⁺ ^{f)}	3 ⁻
2 038.2 \pm 2.1	10 488	60		< 0.5			
2 075.1 \pm 3.0	10 523	50		7.1 \pm 2.0			
2 110.6 \pm 2.1	10 558	140	150	< 0.5	(γ^a)	2 ⁺	2 ⁺
2 120.7 \pm 2.2	10 568	3.4		< 0.5			
2 146.4 \pm 2.2	10 593	220	225	< 0.5		2 ⁺	2 ⁺
2 167.8 \pm 3.0	10 614	60		2.9 \pm 0.5	(γ^a)	(4 ⁺), 5 ⁻ , 6 ⁺ ^{f)}	
2 171.7 \pm 2.2	10 617	60		< 0.5		3 ⁻	
2 206.5 \pm 2.7	10 651	1 000	1 170	2.0 \pm 0.5		0 ⁺ , 1 ⁻ , 2 ⁺	2 ⁺
2 219.3 \pm 2.2	10 664	40		< 0.5		0 ⁺ , 1 ⁻ , 2 ⁺	
2 229.8 \pm 2.3	10 674	19	200	< 0.5	(γ^a)	3 ⁻ , 4 ⁺	2 ⁺
2 258.4 \pm 2.3	10 702	80		< 0.5	(γ^a)	0 ⁺ , 1 ⁻ , 2 ⁺	
2 260.1 \pm 2.5	10 703	190		< 0.5		0 ⁺ , 1 ⁻ , 2 ⁺	
2 296 \pm 10	10 739	340		45 \pm 15	(γ^a)		
2 318.0 \pm 2.3	10 760	160		< 0.5		4 ⁺	
2 321.9 \pm 2.3	10 763	26		< 0.5		4 ⁺	
2 338.5 \pm 2.3	10 780	60		< 0.5		4 ⁺	
2 348.0 \pm 2.5	10 789	13		< 0.5		0 ⁺ , 1 ⁻ , 2 ⁺	
2 375.6 \pm 2.6	10 816	3.7		< 0.5			
2 392.5 \pm 2.4	10 832	31		< 0.5		1 ⁻ , 3 ⁻ , 4 ⁺	

TABLE 1 (continued)

E_p (keV)	$E_x(^{36}\text{Ar})$ (keV)	$(2J+1)I_p I_{\alpha_0}/I'$ (eV)		I' (keV)	Gamma decay	J^π	
		this work	ref. ^{b)}			this work	other work ^{e)}
2 413.1 \pm 2.4	10 852	290	675	< 0.5		2+	2+
2 426 \pm 7	10 864	190		18 \pm 5		(1 ⁻ , 3 ⁻), 4 ⁺ ^{t)}	
2 464.3 \pm 3.0	10 902	390	1 890	1.2 \pm 0.5		1 ⁻	2+
2 479.8 \pm 2.7	10 917	7		< 0.5			
2 497.1 \pm 2.7	10 934	7	970	< 0.5			1 ⁻ , 2+
2 501.7 \pm 2.7	10 938	5		< 0.5			
2 524.0 \pm 2.5	10 960	830		< 0.5		2+	
2 540.4 \pm 2.5	10 976	150		< 0.5		4+	
2 558.2 \pm 2.5	10 993	70		< 0.5		0 ⁺ , 1 ⁻ , 2 ⁺	
2 595.4 \pm 3.0	11 029	800	1 550	1.0 \pm 0.5		2+	2+
2 609.8 \pm 2.6	11 043	160	1 036	< 0.5		4+	0 ⁻
2 616.4 \pm 3.0	11 050	500		0.9 \pm 0.5		0 ⁺ , 1 ⁻ , 2 ⁺	
2 629.8 \pm 3.0	11 063	410	518	1.3 \pm 0.5		1 ⁻ , 3 ⁻	2+
2 658.1 \pm 2.8	11 090	24		< 0.5		4 ⁺ , (5 ⁻) ^{t)}	
2 677.6 \pm 2.8	11 109	25	355	< 0.5		0 ⁺ , 1 ⁻ , 2 ⁺ , 3 ⁻	1 ⁻ , 2+
2 688.3 \pm 3.5	11 120	110		5.5 \pm 1.5			
2 691.6 \pm 2.6	11 123	260		< 0.5		3 ⁻	
2 703.8 \pm 2.7	11 135	430	756	< 0.5		1 ⁻ , 3 ⁻	2+
2 729.4 \pm 3.0	11 160	420	1 185	1.1 \pm 0.5		2+	1 ⁻ , 2+
2 777.0 \pm 2.9	11 206	13	493	< 0.5			1 ⁻
2 780.9 \pm 2.7	11 210	900		< 0.5			
2 795.3 \pm 3.0	11 224	460	2 300	1.0 \pm 0.5		1 ⁻ , 2 ⁺	2+
2 814.4 \pm 3.0	11 242	4000		1.6 \pm 0.5		(1 ⁻) ^{g)}	3 ⁻
2 820.2 \pm 3.0	11 248	290	5 800	< 0.5			
2 850.5 \pm 2.8	11 277	220		< 0.5		3 ⁻	
2 877.0 \pm 3.0	11 303	11		< 0.5			
2 885.8 \pm 2.8	11 312	150		< 0.5		4 ⁺ , 5 ⁻	0 ⁺ , 2 ⁺
2 913.4 \pm 3.0	11 339	90		0.8 \pm 0.5	γ ^{a)}	2+	
2 919.1 \pm 3.0	11 344	140		< 0.5		1 ⁻	

a) Ref. ²⁾, $^{35}\text{Cl}(p, \gamma)^{36}\text{Ar}$ reaction.

b) Ref. ¹⁴⁾, $^{35}\text{Cl}(p, \gamma)^{36}\text{Ar}$ reaction.

c) Ref. ¹⁾, $^{32}\text{S}(\alpha, \gamma)^{36}\text{Ar}$ reaction.

d) Ref. ³⁾, $^{35}\text{Cl}(p, \gamma)^{36}\text{Ar}$ reaction.

e) The results in this column are from ref. ⁵⁾, unless mentioned differently.

f) The χ^2_{min} value of the bracketed J^π assignment slightly exceeds the 0.1 % probability limit; the J^π assignment is thus formally excluded. It is still presented in this case, because the χ^2_{min} value of the unbracketed J^π assignment is only slightly smaller than the 0.1 % probability limit.

g) All J^π assignments are formally excluded by the χ^2 criterion for this resonance; the bracketed J^π assignment has the lowest χ^2_{min} value which only slightly exceeds the 0.1 % probability limit.

h) The identity of this resonance with the 1 637 keV (p, γ) resonance from ref. ²⁾ is doubtful, because at least three strongly interfering (p, p) resonances between 1634 keV and 1638 keV are seen in recent (p, p) work ¹⁵⁾.

The purpose of the simultaneous measurement of the α_0 and γ -ray yields was to decide which compound states emit both γ -rays and α_0 particles. Resonance energies, corresponding ^{36}Ar excitation energies, resonance strengths and widths are listed in the

first five columns of table 1. Relativistically corrected resonance energies are listed in column 1. For the energy calibration the $^{27}\text{Al}(\text{p}, \gamma)^{28}\text{Si}$ resonance at $E_p = 991.90 \pm 0.04$ keV [ref. ⁹)] and the $^{27}\text{Al}(\text{p}, \alpha_0)^{24}\text{Mg}$ resonances at $E_p = 1\,183.3 \pm 0.3$, $1\,364.8 \pm 0.5$ and $1\,381.3 \pm 0.3$ keV [ref. ¹⁰)] were used. In general, the resonance energies given by Ern  and Endt ²) are a little (about 1 keV) lower than those in table 1. The excitation energies E_x of the corresponding levels in ^{36}Ar (column 2) are calculated with the Q -value $Q = 8\,506.0 \pm 2.0$ keV [ref. ¹¹)]. Column three lists the resonance strengths $(2J+1)\Gamma_p\Gamma_{\alpha_0}/\Gamma$. The absolute strength of the resonance at $E_p = 1\,637$ keV was determined from the step in the thick-target yield. The strengths of other resonances are found by comparison of the areas under the thin-target resonance peaks with that of the 1 637 keV standard resonance. To control possible distortion of the resonance curve due to target deterioration, the relative ratios of the areas under the thin-target resonance peaks were compared for two different runs and found to be equal within 20 % for all not too weak resonances. The error in the absolute resonance strengths is estimated to be of the order of 30 %. Resonance strengths as measured by the Soviet group ⁵) are listed in column 4; their values are on the average 40 % higher than those given in column 3. The information on the level widths of some broad resonances, given in column 5, can be extracted from a plot of the measured resonance widths versus proton energy. Fig. 4 shows that most widths (open circles) lie within a smooth strip; the dashed curve is interpreted as the instrumental width Γ_i . For resonances where the measured width Γ_m is indicated by a dot, the natural width Γ was estimated by using the linear relation $\Gamma = \Gamma_m - \Gamma_i$. This relation is justified in ref. ¹²).

Column 6 indicates the resonances at which γ -ray emission has been observed. The symbol γ is used only if during the same run the (p, γ) and (p, α_0) resonance energies were found to be identical within the experimental error. Otherwise, brackets are used to indicate that the assignment is probable but not certain. For a detailed discussion, see subsect. 5.1.

4. Analysis and conclusions from angular-distribution measurements

In both reactions $^{37}\text{Cl}(\text{p}, \alpha_0)^{34}\text{S}$ and $^{35}\text{Cl}(\text{p}, \alpha_0)^{32}\text{S}$, the spin and parity of the target nucleus ground state is $J^\pi = \frac{3}{2}^+$, whereas the α_0 groups populate a 0^+ ground state. Hence the method of analysis of angular-distribution measurements is exactly the same for the two reactions. It was fully described in ref. ⁸).

The analysis can be performed, as in ref. ⁸), with the following restrictions:

- (i) only resonances of natural parity can be excited;
- (ii) there is no orbital momentum mixing in the α_0 channel;
- (iii) in the incoming proton channel, channel spins $s = 1$ and $s = 2$ are possible; the channel spin mixing ratio τ is defined as the intensity in the lowest spin channel over the total intensity in both channels;
- (iv) resonance spins larger than 6 can be excluded;

(v) for resonance states with $J^\pi = 0^+, 5^-$ and 6^+ , only one proton orbital momentum value can contribute; for $J^\pi = 1^-, 2^+, 3^-$ and 4^+ , only the two lowest orbital momenta can contribute; ε is defined as the ratio of amplitudes corresponding to the higher and lower orbital momentum, respectively.

The theoretical angular distribution $W(\theta)$ written as a function of J , ε and τ has to be compared with the observed angular distribution $W(\theta_i)_{\text{exp}}$ in the centre-of-mass system. The search for the best values of the parameters τ and ε was performed by

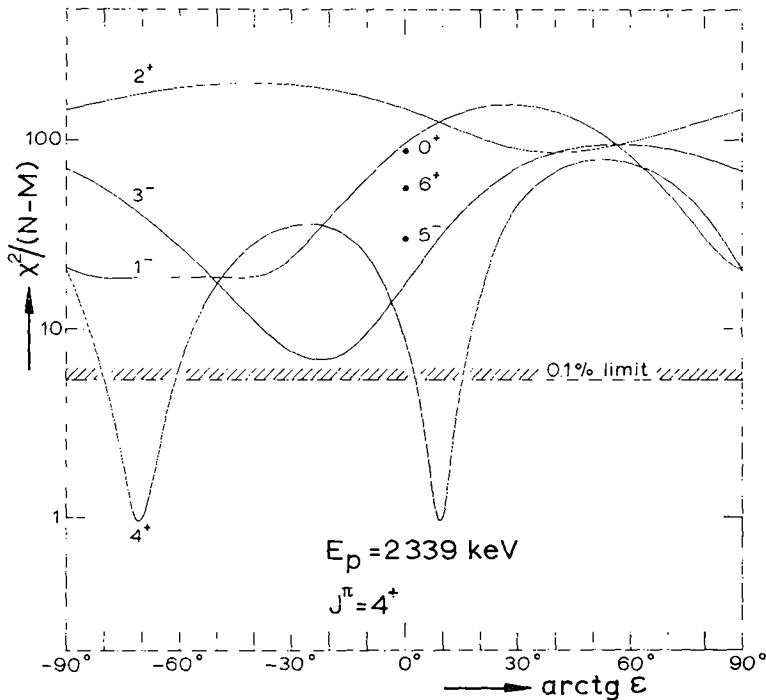


Fig. 5. Values of $\chi^2/(N-M)$ from the angular distribution measurement at the $E_p = 2339$ keV resonance, plotted against the orbital momentum mixing ratio, with J^π as a discrete parameter. The minimalization of χ^2 with respect to the channel spin mixing ratio τ has already been performed. The $J^\pi = 4^+$ assignment is unique but the two equally low χ^2 minima reflect the fact that two possibilities for resonance formation remain.

calculating the function

$$\chi^2 = \sum_i g_i \{W(\theta_i)_{\text{exp}} - W(\theta_i)\}^2,$$

where the g_i are the statistical weights of the observations $W(\theta_i)_{\text{exp}}$. From a contour plot of $\chi^2/(N-M)$ in the (τ, ε) plane, where N is the number of observational angles and M the number of continuously variable parameters, the value of $\chi^2_{\text{min}}/(N-M)$ can be found for a certain assumption of the resonance spin[†]. An example is given

[†] In a latter stage of the investigation, a more efficient computer program developed by R. J. de Meijer considerably accelerated the analysis.

TABLE 2

Values of $\chi^2_{\text{min}}/(N-M)$ for angular distribution measurements at different resonance energies E_p and for different J^π assumptions

E_p (keV)	J^π						
	0 ⁺	1 ⁻	2 ⁺	3 ⁻	4 ⁺	5 ⁻	6 ⁺
873	8.8	<u>1.1</u>	<u>1.1</u>	5.4	14.8	41.2	69.6
883	192	2.2	10.1	524	744	1 268	1 649
968	15.9	<u>1.4</u>	<u>1.2</u>	<u>2.5</u>	14.8	37.0	61.6
986	4.0	<u>3.5</u>	<u>3.5</u>	<u>29.7</u>	62.0	84.9	112
1 119	7.0	<u>3.9</u>	<u>3.7</u>	99.9	198	218	280
1 193	115	<u>2.0</u>	25.7	<u>2.5</u>	22.2	89.7	153
1 231	<u>1.1</u>	<u>0.6</u>	<u>0.7</u>	31.4	53.3	99.1	142
1 264	39.6	<u>2.1</u>	10.2	<u>0.7</u>	<u>3.4</u>	28.7	54.4
1 423	10.0	<u>2.0</u>	<u>1.7</u>	26.6	44.8	75.5	102
1 436	50.8	20.7	30.4	19.8	<u>3.4</u>	5.4	14.9
1 518	78.8	<u>2.8</u>	38.8	<u>3.7</u>	15.6	60.3	93.6
1 528	5.5	<u>1.0</u>	<u>0.7</u>	224	357	505	600
1 582	23	<u>3.0</u>	<u>0.8</u>	59.0	222	226	274
1 588	486	18.3	214	<u>3.6</u>	116	258	486
1 637	81.1	<u>0.8</u>	45.3	<u>1.0</u>	39.2	81.6	129
1 709	23.1	<u>4.4</u>	14.3	<u>4.4</u>	7.3	22.0	35.2
1 715	8.2	<u>2.8</u>	<u>1.4</u>	23.5	77.2	96.5	128
1 804 ^{a)}	<u>3.1</u>	<u>2.6</u>	<u>2.6</u>	<u>1.1</u>	4.9	7.3	9.9
1 813	30.2	<u>0.8</u>	21.5	65.1	88.0	163	208
1 847	36.3	10.3	18.2	8.1	5.7	16.4	32.4
1 867	37.5	18.0	<u>0.4</u>	161	294	351	448
1 988	4.2	<u>0.5</u>	<u>0.3</u>	159	261	343	406
2 038	152	131	152	5.1	<u>3.3</u>	213	274
2 111	36.9	53.0	<u>1.0</u>	169	207	202	266
2 146	16.0	11.8	<u>2.0</u>	17.9	67.1	132	167
2 168	22.9	11.2	16.6	7.9	<u>2.9</u>	<u>1.8</u>	<u>2.5</u>
2 172	68.8	67.4	52.7	<u>0.9</u>	122	96.4	115
2 207	<u>3.4</u>	<u>3.8</u>	<u>3.2</u>	40.9	72.5	106	131
2 219	<u>3.5</u>	<u>2.5</u>	<u>0.5</u>	63.1	84.9	109	130
2 230	13.4	12.6	14.2	<u>4.0</u>	<u>5.1</u>	15.3	20.8
2 258	<u>2.5</u>	<u>1.5</u>	<u>0.9</u>	13.0	31.6	67.9	101
2 260	<u>2.7</u>	<u>1.3</u>	<u>0.9</u>	56.4	116	230	325
2 318	86.2	19.1	90.1	11.1	<u>0.2</u>	11.2	27.3

TABLE 2 (continued)

E_p (keV)	J^π						
	0 ⁺	1 ⁻	2 ⁺	3 ⁻	4 ⁺	5 ⁻	6 ⁺
2 322	89.6	16.5	82.7	12.9	<u>1.6</u>	8.6	26.1
2 339	87.8	18.5	87.3	6.9	<u>1.0</u>	30.3	56.3
2 348	<u>2.9</u>	<u>2.5</u>	<u>2.5</u>	17.5	35.5	38.5	45.9
2 393	13.5	<u>1.9</u>	9.8	<u>0.5</u>	<u>4.5</u>	6.9	12.9
2 413	58.3	88.7	<u>1.3</u>	17.1	76.9	203	236
2 426	20.6	5.5	21.5	5.1	<u>4.4</u>	8.7	13.2
2 464	76.2	<u>4.4</u>	61.7	238	293	332	359
2 524	91.1	11.1	<u>3.6</u>	143	341	729	1 024
2 540	80.3	31.5	76.4	18.7	<u>2.3</u>	5.8	15.7
2 558	<u>0.2</u>	<u>0.2</u>	<u>0.3</u>	44.1	74.8	109	133
2 595	133	176	<u>0.6</u>	41.6	285	731	874
2 610	114	19.2	114	16.1	<u>3.2</u>	8.1	25.5
2 616	<u>3.1</u>	<u>1.1</u>	<u>1.2</u>	106	174	242	288
2 630	58.0	<u>2.9</u>	43.0	<u>2.3</u>	15.3	54.0	87.0
2 658	65.0	13.2	59.3	11.3	<u>4.6</u>	6.2	14.3
2 678	<u>3.6</u>	<u>0.9</u>	<u>1.6</u>	<u>3.1</u>	7.4	16.1	26.4
2 692	40.0	19.6	16.9	4.3	92.1	137	189
2 704	96.8	<u>1.9</u>	75.8	<u>1.8</u>	18.0	68.1	111
2 729	11.3	8.4	<u>3.8</u>	136	190	215	254
2 795	16.1	<u>0.5</u>	<u>1.5</u>	127	187	324	372
2 814 ^{b)}	386	4.8	249	31.2	44.2	83.2	148
2 851	173	124	146	<u>0.7</u>	14.6	248	302
2 886	168	40.2	137	22.4	<u>0.8</u>	<u>3.8</u>	22.9
2 913	8.3	10.9	<u>0.5</u>	48.9	69.7	103	149
2 919	23.8	<u>3.9</u>	7.3	23.5	51.0	123	196

^{a)} Poor statistics.

^{b)} For discussion, see text.

in fig. 5. A spin assumption is excluded if the value of $\chi^2_{\min}/(N-M)$ exceeds the 0.1 % probability limit; the values of $\chi^2_{\min}/(N-M)$ for different resonances and different spin assumptions are listed in table 2. Underlined numbers indicate possible solutions. Analysis of all not too weak resonances yielded at least one J^π solution. An exception is the 2 814 keV resonance for which no J^π assumption led to a χ^2 value below the 0.1 % probability limit. This is not well understood; one may seek an explanation in possible interference with the weaker 2 820 keV resonance or with another unknown

TABLE 3
Spins, formation and population parameters in the $^{35}\text{Cl}(p, \alpha_0)^{32}\text{S}$ reaction

E_p (keV)	J^π	τ		$\arctg \varepsilon(\text{deg})$		$p(1)$ $\times 10^3$	$p(2)$ $\times 10^3$
		set I	set II	set I	set II		
873	1 ⁻					530 \pm 22	
	2 ⁺	0.26 \pm 0.03	0.05 \pm 0.04	+63 \pm 5	+19 \pm 4	488 \pm 29	231 \pm 28
883	1 ⁻					903 \pm 6	
968	1 ⁻					485 \pm 21	
	2 ⁺	0.18 \pm 0.04		+40 \pm 7		530 \pm 30	173 \pm 11
	3 ⁻	0.204 \pm 0.028	0.04 \pm 0.03	+47 \pm 6	-22 \pm 5	420 \pm 40	360 \pm 30
986	1 ⁻					731 \pm 25	
	2 ⁺	0.28 \pm 0.03	0.00 \pm 0.04	-78 \pm 4	- 8.5 \pm 5.0	360 \pm 30	480 \pm 50
1 119	1 ⁻					613 \pm 8	
	2 ⁺	0.305 \pm 0.015	0.025 \pm 0.020	+79 \pm 2	+ 8 \pm 2	442 \pm 14	330 \pm 15
1 193	1 ⁻	0.00 \pm 0.03		+75 \pm 5		415 \pm 10	
	3 ⁻	0.005 \pm 0.020		0 \pm 8		460 \pm 11	284 \pm 6
1 231	1 ⁻					636 \pm 16	
	2 ⁺	0.284 \pm 0.024	0.000 \pm 0.024	+82.0 \pm 3.5	+ 5.0 \pm 2.5	412 \pm 23	363 \pm 24
1 266	1 ⁻	0.00 \pm 0.06		-85 \pm 15		396 \pm 23	
	3 ⁻	0.09 \pm 0.04		- 3 \pm 8		505 \pm 21	260 \pm 11
	4 ⁺	0.372 \pm 0.024	0.09 \pm 0.04	-73 \pm 5	+22 \pm 3	436 \pm 29	370 \pm 30
1 423	1 ⁻					563 \pm 14	
	2 ⁺	0.21 \pm 0.03	0.02 \pm 0.04	+60 \pm 4	+22 \pm 4	441 \pm 24	282 \pm 18
1 436	4 ⁺	0.23 \pm 0.03	0.06 \pm 0.04	-37.0 \pm 4.5	- 8 \pm 6	514 \pm 24	190 \pm 22
1 518	1 ⁻	0.00 \pm 0.03		-75 \pm 10		405 \pm 23	
	3 ⁻	0.020 \pm 0.020		+ 4 \pm 6		463 \pm 16	289 \pm 17
1 528	1 ⁻					703 \pm 7	
	2 ⁺	0.309 \pm 0.013	0.027 \pm 0.015	-80.5 \pm 2.5	- 7 \pm 2	392 \pm 12	434 \pm 14
1 582	1 ⁻					791 \pm 10	
	2 ⁺	0.085 \pm 0.020		-39 \pm 3		278 \pm 21	588 \pm 17
1 588	3 ⁻	0.000 \pm 0.007		-20.0 \pm 1.5		472 \pm 7	292 \pm 4
1 637	1 ⁻	0.03 \pm 0.05		+85 \pm 10		423 \pm 10	
	3 ⁻	0.175 \pm 0.020	0.000 \pm 0.017	-40 \pm 3	+ 8 \pm 4	441 \pm 18	312 \pm 17
1 709	1 ⁻	0.00 \pm 0.04		-70 \pm 15		330 \pm 40	
	3 ⁻	0.26 \pm 0.05	0.007 \pm 0.005	-44 \pm 7	+ 9 \pm 8	480 \pm 40	290 \pm 40
1 715	1 ⁻					578 \pm 12	
	2 ⁺	0.288 \pm 0.022	0.113 \pm 0.027	+60.5 \pm 4.5	+22 \pm 4	485 \pm 20	276 \pm 15
1 813	1 ⁻					871 \pm 23	
1 847	(4 ⁺)	0.26 \pm 0.03		-66 \pm 3		380 \pm 30	348 \pm 28
1 867	2 ⁺	0.003 \pm 0.017		-40.0 \pm 2.5		222 \pm 18	616 \pm 14
1 988	1 ⁻					708 \pm 9	
	2 ⁺	0.275 \pm 0.015	0.000 \pm 0.015	-76 \pm 3	-10.5 \pm 2.0	367 \pm 13	455 \pm 12
2 038	(3 ⁻)	0.660 \pm 0.020	0.520 \pm 0.025	-68 \pm 7	-17 \pm 5	712 \pm 21	183 \pm 20
	4 ⁺	0.210 \pm 0.020		+53 \pm 3		310 \pm 23	589 \pm 20
2 111	2 ⁺	0.096 \pm 0.014		+79.0 \pm 2.5		255 \pm 14	467 \pm 14
2 146	2 ⁺	0.24 \pm 0.02		+28 \pm 7		541 \pm 22	253 \pm 10
2 168	4 ⁺	0.07 \pm 0.04		-25 \pm 5		490 \pm 30	142 \pm 9
2 172	3 ⁻	0.107 \pm 0.018		+77 \pm 5		165 \pm 18	625 \pm 13
2 207	1 ⁻					613 \pm 15	
	2 ⁺	0.315 \pm 0.025	0.05 \pm 0.04	+76 \pm 6	+ 9 \pm 5	443 \pm 24	346 \pm 23

TABLE (continued)

E_p (keV)	J^π	τ		$\arctg \varepsilon(\text{deg})$		$p(1)$ $\times 10^3$	$p(2)$ $\times 10^3$
		set I	set II	set I	set II		
2 219	1 ⁻					716 \pm 15	
	2 ⁺	0.215 \pm 0.025	0.000 \pm 0.013	-71 \pm 6	-19 \pm 5	327 \pm 23	493 \pm 20
2 230	3 ⁻	0.44 \pm 0.07		-22 \pm 11		680 \pm 50	142 \pm 19
	4 ⁺	0.39 \pm 0.06	0.05 \pm 0.06	-87 \pm 7	+25 \pm 5	400 \pm 60	440 \pm 60
2 258	1 ⁻					611 \pm 19	
	2 ⁺	0.34 \pm 0.03	0.12 \pm 0.04	+67 \pm 8	+16 \pm 7	490 \pm 30	306 \pm 25
2 260	1 ⁻					633 \pm 10	
	2 ⁺	0.324 \pm 0.017	0.062 \pm 0.023	+76 \pm 5	+ 9.5 \pm 3.5	448 \pm 12	400 \pm 17
2 318	4 ⁺	0.26 \pm 0.04	0.000 \pm 0.023	-59 \pm 3	+ 2 \pm 2	464 \pm 19	256 \pm 21
2 322	4 ⁺	0.310 \pm 0.020	0.010 \pm 0.030	-56 \pm 3	- 1 \pm 2	483 \pm 20	230 \pm 20
2 339	4 ⁺	0.305 \pm 0.025	0.000 \pm 0.008	-70 \pm 3	+ 8 \pm 2	424 \pm 18	327 \pm 24
2 348	1 ⁻					732 \pm 22	
	2 ⁺	0.22 \pm 0.04	0.04 \pm 0.05	-60 \pm 10	-24 \pm 8	340 \pm 50	490 \pm 40
2 393	1 ⁻					420 \pm 30	
	3 ⁻	0.115 \pm 0.016		-44 \pm 3		401 \pm 21	295 \pm 18
	4 ⁺	0.30 \pm 0.04	0.00 \pm 0.04	-64 \pm 5	+ 4 \pm 4	445 \pm 25	286 \pm 29
2 413	2 ⁺	0.609 \pm 0.020	0.488 \pm 0.028	+65 \pm 9	+15 \pm 8	699 \pm 20	180 \pm 16
2 426	(1 ⁻)	0.00 \pm 0.03		-60 \pm 10		150 \pm 80	
	(3 ⁻)	0.260 \pm 0.020		-24 \pm 3		581 \pm 14	182 \pm 6
	4 ⁺	0.30 \pm 0.05	0.000 \pm 0.028	-79 \pm 5	+14 \pm 5	380 \pm 40	400 \pm 50
2 464	1 ⁻					880 \pm 10	
2 524	2 ⁺	0.348 \pm 0.010	0.088 \pm 0.014	-78.0 \pm 3.5	- 8.0 \pm 2.5	435 \pm 10	395 \pm 10
2 540	4 ⁺	0.255 \pm 0.025	0.000 \pm 0.010	-54 \pm 4	- 4 \pm 3	471 \pm 19	216 \pm 28
2 558	1 ⁻					672 \pm 14	
	2 ⁺	0.285 \pm 0.025	0.000 \pm 0.020	-88 \pm 7	- 2 \pm 5	390 \pm 20	411 \pm 20
2 595	2 ⁺	0.555 \pm 0.010	0.390 \pm 0.015	+73.5 \pm 4.5	+12 \pm 4	640 \pm 10	223 \pm 9
2 610	4 ⁺	0.285 \pm 0.020	0.000 \pm 0.015	-56 \pm 3	- 3 \pm 2	475 \pm 15	221 \pm 20
2 616	1 ⁻					707 \pm 10	
	2 ⁺	0.280 \pm 0.020	0.040 \pm 0.025	-69 \pm 5	-15 \pm 4	383 \pm 20	445 \pm 17
2 630	1 ⁻					410 \pm 14	
	3 ⁻	0.295 \pm 0.020	0.00 \pm 0.03	-61 \pm 5	- 2 \pm 4	451 \pm 23	296 \pm 26
2 658	4 ⁺	0.291 \pm 0.029	0.000 \pm 0.019	-60 \pm 5	0 \pm 4	462 \pm 21	250 \pm 40
2 678	1 ⁻					539 \pm 40	
	2 ⁺	0.15 \pm 0.06		+40 \pm 8		440 \pm 40	316 \pm 26
	3 ⁻	0.32 \pm 0.04		-72 \pm 8		410 \pm 40	370 \pm 50
2 692	3 ⁻	0.270 \pm 0.015	0.000 \pm 0.008	-88.5 \pm 3.0	+26 \pm 2	327 \pm 15	481 \pm 17
2 704	1 ⁻					403 \pm 11	
	3 ⁻	0.265 \pm 0.018	0.013 \pm 0.023	-52 \pm 4	- 2 \pm 3	468 \pm 17	273 \pm 17
2 792	2 ⁺	0.160 \pm 0.020	0.000 \pm 0.015	-60 \pm 15	-28 \pm 4	300 \pm 21	581 \pm 16
2 795	1 ⁻					758 \pm 12	
	2 ⁺	0.13 \pm 0.03		-40 \pm 5		340 \pm 30	495 \pm 23
2 814	(1 ⁻)	0.00 \pm 0.03		-60 \pm 10		274 \pm 10	
2 851	3 ⁻	0.717 \pm 0.019		-50 \pm 9		800 \pm 23	99 \pm 22
2 886	4 ⁺	0.267 \pm 0.018	0.007 \pm 0.025	-49 \pm 3	- 7 \pm 2	497 \pm 17	178 \pm 18
2 913	2 ⁺	0.154 \pm 0.021		+76 \pm 5		306 \pm 23	350 \pm 17
2 919	1 ⁻					549 \pm 10	

but very broad resonance. One still might consider the $J^\pi = 1^-$ assignment to the 2 814 keV resonance as the most probable one because the corresponding χ^2 value is the only one very near the 0.1 % probability limit.

The values and errors of the formation parameters τ and ε were used to determine the population parameters $p(m)$. An exception is the case $J^\pi = 1^-$. Here, τ and ε cannot be uniquely determined, so population parameters were extracted directly from a population parameter analysis as described in ref. 8). The results are summarized in table 3. In some cases, one spin assumption allows two different possibilities for the formation of the resonant state. In such cases, the two different sets of possible

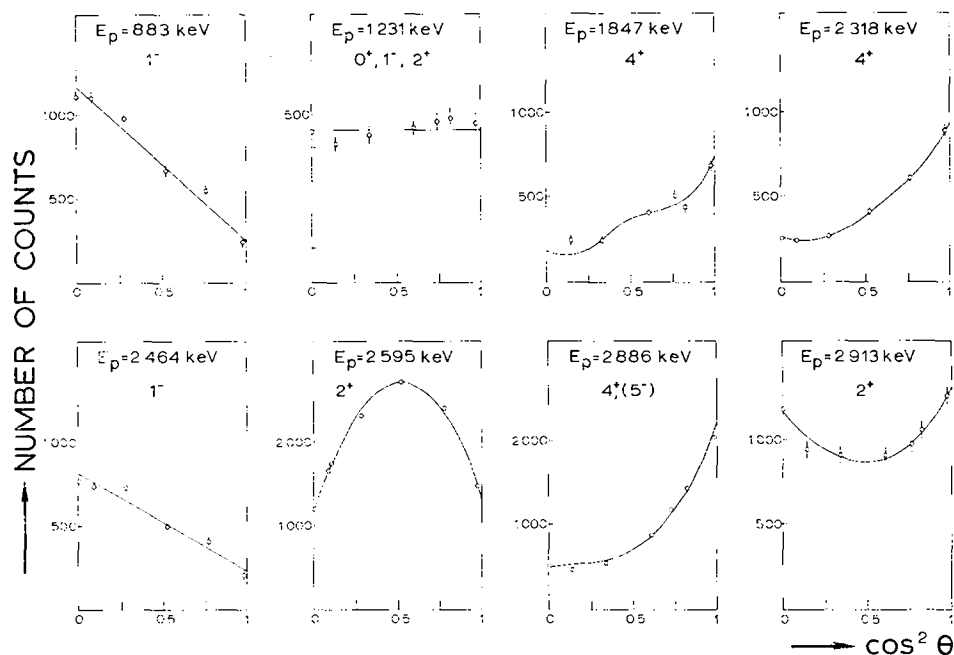


Fig. 6. Typical angular distributions of the α -particles at eight different resonances. The solid lines give the best fit on the basis of the channel spin formalism.

formation parameters (labelled as I and II) correspond to the one common, uniquely determined set of population parameters.

From the analysis, the spin was uniquely determined for 21 resonances. In 16 cases, two different J^π assumptions are consistent with the measurements. The isotropic angular distributions at eight resonances allow spin assignments of 0^+ , 1^- and 2^+ . Best fits of some of the angular distributions are given in fig. 6. The resonances with possible $J^\pi = 3^-$ assignments form an interesting group, the properties of which will be discussed in subject. 5.4. The angular distributions of these resonances are presented in fig. 7.

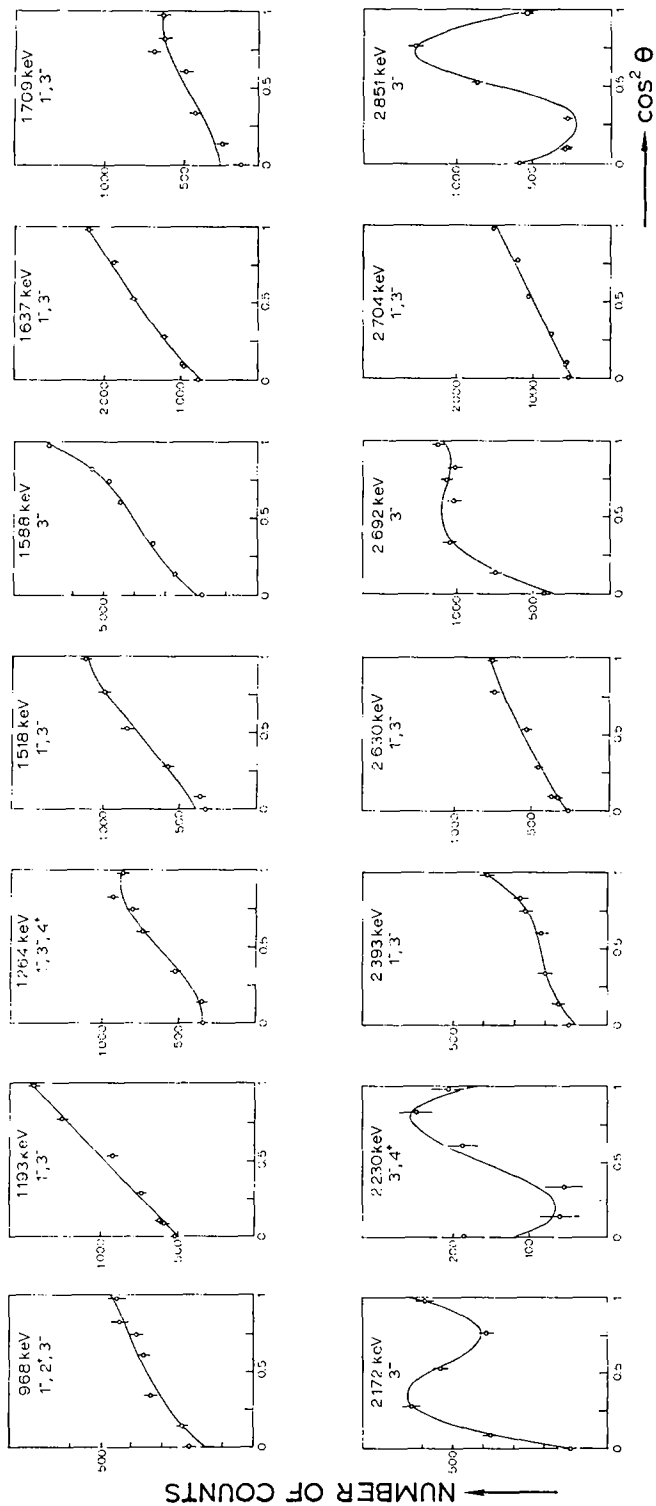


Fig. 7. Angular distributions of all resonances for which the $J^\pi = 3^-$ assignment is possible on the basis of the (p, α_0) work.

5. Discussion of the results

5.1. THE EXCITATION CURVE

Properties of the resonances determined in the present investigation were partly known from previous work. Earlier data are reviewed by Endt and van der Leun¹³⁾. Here, the present data will be compared only with some of the most recent work.

Resonances in the $^{35}\text{Cl}(\text{p}, \gamma)^{36}\text{Ar}$ reaction are reported in refs. ^{1,2,14)}. Resonance states, which decay by both α_0 and γ -emission, are listed in table 1, column 6.

All resonances found by the Soviet group⁵⁾ in the $^{35}\text{Cl}(\text{p}, \alpha_0)^{32}\text{S}$ reaction for proton energies $1.56 \leq E_p \leq 2.91$ MeV could be identified or resolved into doublets in the present investigation. Moreover, about 25 new resonances were discovered in the same energy region.

If one compares the reactions $^{37}\text{Cl}(\text{p}, \alpha_0)^{34}\text{S}$ [ref. ⁸⁾] and $^{35}\text{Cl}(\text{p}, \alpha_0)^{32}\text{S}$, one observes in the latter reaction more broad resonances and a lower resonance density. Preliminary measurements¹⁵⁾ have shown that some of the broad resonances show a considerable width for inelastic proton scattering. This may be due to the fact that the excitation energy of the first excited state in ^{35}Cl is lower ($E_x = 1.22$ MeV) than in ^{37}Cl ($E_x = 1.72$ MeV).

The lower level density ρ can be readily explained by the lower excitation energy E_x in the compound nucleus ^{36}Ar ($E_x = 9.5-11.5$ MeV). Taking into account losses due to finite energy resolution [see ref. ⁸⁾], we find $\rho_{\text{exp}} = 43 \text{ MeV}^{-1}$ at $E_x = 10.6$ MeV. Under the assumption that all natural parity resonances with $J \leq 4$ are detected, this result is compared with the corresponding semi-empirical predictions of Newton¹⁶⁾ and of Gilbert, Chen and Cameron¹⁷⁾ by a procedure described in ref. ⁸⁾. The predicted values, supposed to be correct within a factor of three, are $\rho_{\text{pred}}(\text{Newton}) = 51 \text{ MeV}^{-1}$ and $\rho_{\text{pred}}(\text{Gilbert}) = 62 \text{ MeV}^{-1}$, both in good agreement with the measured value.

5.2. SPIN ASSIGNMENTS

To some resonances, spins and parities were assigned previously by Ern   *et al.*^{1,3)} and by Karad  ev *et al.*⁵⁾. The results of these authors in table 1, column 8, are on the whole in good agreement with those of the present study.

An interesting case is the resonance at 2 595 keV. At that energy, Ern  ³⁾ found a resonance to which he assigned $J^\pi = 3^+$. At nominally the same energy, a resonance is also found from the (p, α_0) work, but with a J^π assignment of $J^\pi = 2^+$. To resolve the contradiction, the (p, γ) and (p, α_0) yields were measured simultaneously. The result (fig. 8) shows that the (p, γ) and (p, α) resonances have different energies. The fact that the (p, γ) resonance does not possess a measurable α_0 width is in agreement with the assignment $J^\pi = 3^+$.

For some resonances, information available on the γ -decay to bound states in ^{36}Ar (see ref. ²⁾, table 1) may impose restrictions on possible J^π values. These cases are collected in table 4, where also the argumentation is to be found leading to J^π rejection. The number of unique spin assignments is thus increased by three.

Interesting is also the formation of the resonances. In the reactions $^{37}\text{Cl}(p, \alpha_0)^{34}\text{S}$ [ref. ⁸)] and $^{41}\text{K}(p, \alpha_0)^{38}\text{Ar}$ [ref. ¹⁸)], a number of $J^\pi = 1^-$ resonances were found, which were formed almost purely via channel spin 1. No such cases were found in the reaction $^{35}\text{Cl}(p, \alpha_0)^{32}\text{S}$.

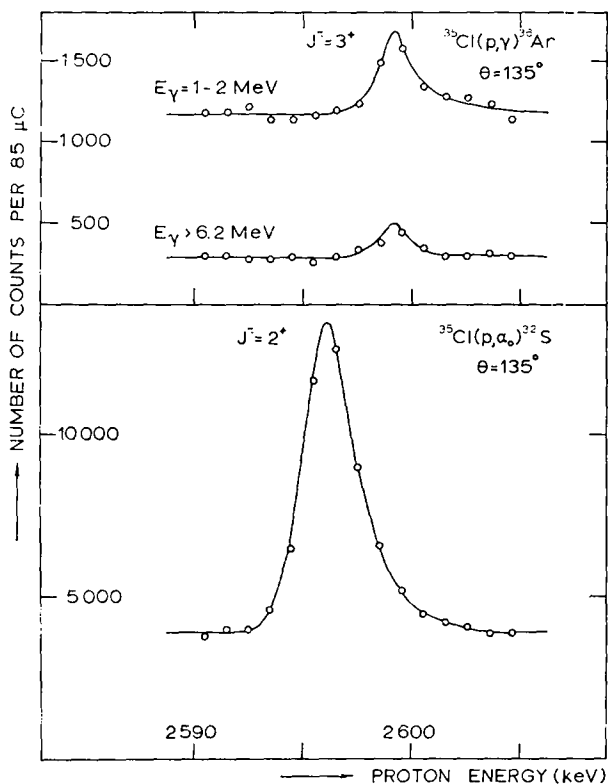


Fig. 8. The yields of the $^{35}\text{Cl}(p, \gamma)^{36}\text{Ar}$ and the $^{35}\text{Cl}(p, \alpha_0)^{32}\text{S}$ reactions in the neighbourhood of the $E_p = 2595$ keV doublet, measured simultaneously.

TABLE 4

Spin-parity assignments in ^{36}Ar from combining $^{35}\text{Cl}(p, \alpha_0)^{32}\text{S}$ and $^{35}\text{Cl}(p, \gamma)^{36}\text{Ar}$ [ref. ²)] results

E_p (keV)	$E_x(^{36}\text{Ar})$ (keV)	J^π	
		(p, α_0) work	combining (p, α_0) work and (p, γ) resonance branching
986	9 464	$(0^+, 1^-, 2^+)$	$1^-, 2^+{}^a)$
1 436	9 902	$4^+, (5^-)$	$4^+{}^b)$
1 518	9 981	$1^-, 3^-$	$1^-{}^b)$
1 709	10 167	$1^-, 3^-$	$3^-{}^b)$
2 258	10 702	$0^+, 1^-, 2^+$	$1^-, 2^+{}^a)$

^a) The rejected J^π value would have led to a $0^+ \rightarrow 0^+$ γ -transition.

^b) The rejected J^π values would have led to E3 transitions with a strength of at least 100 W.u.

On the other hand, in the present investigation several $J^\pi = 3^-$ resonances were found, formed preferentially through the angular momentum $l_p = 3$. A discussion in terms of analogue states is given in subsect. 5.4.

5.3. PARTIAL WIDTHS

The resonances at $E_p = 873, 968$ and 986 keV have been excited through the three reactions (p, γ) [ref. ¹⁾], (α, γ) [ref. ¹⁾] and (p, α_0) . From the corresponding yield measurements, unique determinations of the partial widths $(2J+1)\Gamma_p$, $(2J+1)\Gamma_\gamma$ and $(2J+1)\Gamma_{\alpha_0}$ can be obtained. The results are summarized in table 5. For all three resonances, the proton width is larger than the α_0 width by an order of magnitude. For the 873 keV, $J^\pi = 2^+$ resonance, this behaviour is readily explained by the fact that, in spite of the positive reaction Q -value, the penetration for s-wave protons is much larger than that for d-wave α_0 particles. The interpretation of the 968 keV resonance as analogue state (see subsect. 5.4) would explain the relatively large proton width in this case.

TABLE 5

Energies, strengths and partial widths of three resonances excited through the three reactions (p, γ) , (α, γ) and (p, α_0)

E_p (keV)	$E_\alpha^a)$ (keV)	E_x (keV)	$(2J+1)\frac{\Gamma_p\Gamma_\gamma^a)}{F}$ (eV)	$(2J+1)\frac{\Gamma_{\alpha_0}\Gamma_\gamma^a)}{F}$ (eV)	$(2J+1)\frac{\Gamma_p\Gamma_{\alpha_0}}{F}$ (eV)	$(2J+1)\Gamma_p$ (eV)	$(2J+1)\Gamma_{\alpha_0}$ (eV)	$(2J+1)\Gamma_\gamma$ (eV)
873	3 056	9 355	0.5	0.05	1.2	13.7	1.4	0.6
968	3 161	9 447	0.5	0.15	1.8	8.3	2.5	0.7
986	3 182	9 464	2.5	0.05	0.5	28.0	0.6	2.8

^{a)} Ref. ¹⁾.

Unfortunately, the $^{32}\text{S}(\alpha, \gamma)^{36}\text{Ar}$ reaction was not studied at energies higher than $E_\alpha = 3 182$ keV. Therefore, for resonances in the $^{35}\text{Cl}(\text{p}, \alpha_0)^{32}\text{S}$ reaction with $E_p > 986$ keV, only lower estimates for Γ_p and Γ_{α_0} can be given. An exception is the $1 588$ keV $J^\pi = 3^-$ resonance, which was investigated recently with the $^{35}\text{Cl}(\text{p}, \text{p})^{35}\text{Cl}$ reaction ¹⁵⁾. The preliminary analysis yields a proton width $\Gamma_p = 300 \pm 80$ eV, which, together with the (p, α_0) resonance strength, leads to an α -particle width $\Gamma_{\alpha_0} = 40 \pm 15$ eV.

5.4. ANALOGUE STATES

Excited states of ^{36}Cl have been investigated by Hoogenboom *et al.* ¹⁹⁾ with the $^{35}\text{Cl}(\text{d}, \text{p})^{36}\text{Cl}$ reaction. Isobaric analogues of excited states in ^{36}Cl with $E_x > 2$ MeV can be expected to appear as resonances in $^{35}\text{Cl} + \text{p}$.

The identification of isobaric analogue states in ^{36}Ar is not easy because of the relatively high density of excited states at low excitation energy in ^{36}Cl , and since the spins of the relevant ^{36}Cl states are known in only very few cases. For simplification, we restrict our discussion to ^{36}Cl bound states with a relatively large f-wave neutron

capture contribution, which appear at excitation energies of $E_x = 2\,472, 2\,522, 2\,816, 2\,868, 3\,103$ and $3\,728$ keV. From a theoretical point of view, these states are interesting as possible $(1d_{3/2})^3 1f_{7/2}$ configurations. Experimentally, they offer the advantage of large relative spacings.

A spin and parity of $J^\pi = 3^-$ was determined for the $E_x = 2\,472$ keV state ^{20). In ref. ²¹⁾, $J^\pi = 3^-, (4^-)$ is assigned to the $2\,868$ keV state. A consideration of the reduced intensity of the primary γ -ray transition from the $J^\pi = 2^+$ neutron capture state to the $2\,868$ keV state ²⁰⁾ excludes the $J^\pi = (4^-)$ assignment to the latter state. The ³⁶Cl reduced neutron widths, published in ref. ¹⁹⁾, were extracted from a PWBA analysis. To get a more realistic picture, we compared the Hoogenboom *et al.* ¹⁹⁾ $(2J+1)\theta_n^2$ data (PWBA) with the $(2J+1)S_n$ data (DWBA) of Rapaport and Buechner ²²⁾ for the lowest excited states in ³⁸Cl, derived in both cases from the study of the ³⁷Cl(d, p)³⁸Cl reaction. Defining θ_0^2 by $\theta_n^2 = \theta_0^2 S_n$, one extracts an average value of $\theta_0^2 = 0.019$ for the $l_n = 3$ components corresponding to the three lowest excited states in ³⁸Cl. This value is in fair agreement with the value $\theta_0^2 = 0.013$, given by Macfarlane and French ²³⁾ for $f_{7/2}$ states in the s-d shell. With the same factor $\theta_0^2 = 0.019$, values of $(2J+1)S_n$ for the $l_n = 3$ states in ³⁶Cl were computed from the data in ref. ¹⁹⁾. These values, listed in table 7, column 3, show that the ³⁶Cl states under consideration have strong single-particle character. We now turn our attention to the resonances in ³⁵Cl+p.}

In table 6, the $l_p = 3$ reduced proton widths are given, as deduced from the present (p, α_0) work. Unfortunately, the data contain more ambiguities than just the unknown factor Γ_{α_0}/Γ . First of all, the formation of a resonance, under a certain assumption for J^π , is not always uniquely determined. For this reason two values of $(2J+1)\theta_p^2$ ($l_p = 3$) Γ_{α_0}/Γ are given for some 3^- resonances and lower limits for some 1^- resonances. Second, for a number of resonances, J^π assignments of both 1^- and 3^- are possible. These ambiguities make the identification of analogue states even more difficult.

To estimate the position of analogue resonances, one needs information on the Coulomb energy difference for the pair of nuclei ³⁶Cl-³⁶Ar. From work of Berg *et al.* ²⁴⁾, it is known that the analogue of the ³⁶Cl ground state has an excitation energy of $E_x = 6\,611.9 \pm 0.9$ keV in ³⁶Ar. This implies a Coulomb energy difference of $\Delta E_C = 6\,683$ keV. This value is in disagreement with Ern 's interpretation ³⁾ of the $E_p = 860$ keV resonance in ³⁵Cl+p as the analogue of the ³⁶Cl state at $E_x = 2\,472$ keV, which would entail $\Delta E_C = 6\,940$ keV. One can now try to find a correspondence between the ³⁶Cl states with $l_n = 3$ and the (p, α_0) resonances listed in table 6. The sequence of ³⁶Cl states at $E_x = 2\,522, 2\,816, 2\,868, 3\,103$ and $3\,728$ keV is astonishingly well reproduced by the sequence of (p, α_0) resonances at $E_p = 968, 1\,193, 1\,264, 1\,588$ and $2\,172$ keV. Moreover, there exists no other sequence of (p, α_0) resonances which fulfills the following conditions: (i) to each ³⁶Cl level with $l_n = 3$ an analogue resonance can be assigned; (ii) all strong f-wave capture resonances can be identified as analogues of ³⁶Cl states. The interpretation of the mentioned reso-

nances as analogue states, however, leads to an average Coulomb energy difference of $\Delta E_C = 6.96$ MeV, which is almost 280 keV higher than the value following from ref. ²⁴). Calculations of the Thomas-Ehrman shift and the electromagnetic shift were

TABLE 6
Reduced f-wave proton widths of $^{35}\text{Cl}(p, \alpha_0)^{32}\text{S}$ resonances

E_p (keV)	$(2J+1)\theta_p^2(\Gamma_{\alpha_0}/\Gamma) \times 10^3$ for $l_p = 3$		
	$J^\pi = 1^-$	$J^\pi = 3^-$	$J^\pi = 5^-$
968	$> 220^d)$	340 ^{a)} or 100 ^{b)}	
1 193	320	1.6	
1 264	60	8	
1 518	14		
1 588		130 ^{c)}	
1 637	> 470	330 or 13	
1 709		24 or 1.2	
2 168			29
2 172		60	
2 230		3.9	
2 393	> 1.9	4.2	
2 630	> 14	46 or 0.06	
2 678	> 0.7		
2 692		30 or 6	
2 704	> 12	23 or 0.7	
2 851		17	
2 886			12

^{a-d)} The factor Γ_{α_0}/Γ is known for these cases (see subject. 5.3); the value $(2J+1)\theta_p^2(l_p = 3) \times 10^3$ amounts to 1 550, 450, 1 120 and $> 1 020$ for ^{a)}, ^{b)}, ^{c)} and ^{d)}, respectively.

TABLE 7
Final conclusions on analogue states in ^{36}Ar

$^{36}\text{Cl}^*$ (keV)	I_n	$S_n^a)$ ($I_n = 3$)	$J^\pi^b)$	E_p in $^{36}\text{Cl}+p$ (keV)	$^{36}\text{Ar}^*$ (keV)	$\theta_p^2;$	$\theta_p^2 \cdot \Gamma_{\alpha_0}/\Gamma$ ($l_p = 3$) ($\times 10^3$)	ΔE_C (keV)
2 472	1(+3)		3-	860	9 342			6 940
2 522	3	1.0	(3-)	968	9 447	220 ^{c)} ;	34	6 996
2 816	3	$\left\{ \begin{smallmatrix} 0.9 \\ 0.40 \end{smallmatrix} \right\}$	$\left\{ \begin{smallmatrix} (1-) \\ (3-) \end{smallmatrix} \right\}$	1 193	9 666	$\left\{ \begin{smallmatrix} ; \\ ; \end{smallmatrix} \right\}$	$\left\{ \begin{smallmatrix} 110 \\ 0.23 \end{smallmatrix} \right\}$	6 921
2 868	3	0.17	3-	1 264	9 735	;	1.1	6 938
3 103	1+3	0.17	(3-)	1 588	10 050	160;	18	7 018
3 728	3	0.17	(3-)	2 172	10 617		9	6 960

^{a)} From ref. ¹⁹), with spectroscopic factors extracted as indicated in text.

^{b)} J^π values are bracketed if deduced on the basis of the present analogue state assignments; see text.

^{c)} Of the two possible values for θ_p^2 , the higher one is chosen, because it is in much better agreement with S_n .

then carried out ¹⁸⁾ to see whether these can explain this discrepancy. One thus finds that the ^{36}Ar - ^{36}Cl Coulomb energy difference for the $(d_{\frac{3}{2}})^3 f_{\frac{7}{2}}$ states under consideration should be about 100 to 300 keV higher than that for the $(d_{\frac{3}{2}})^3 d_{\frac{3}{2}}$ ^{36}Cl ground

state and its analogue with $J^\pi = 2^+, l = 2$. Although the theoretical shifts are strongly dependent on the values of the reduced widths and on the amount of possible $d_{3/2}$ admixture to the ground-state configuration, one can conclude that the observed shift is certainly plausible.

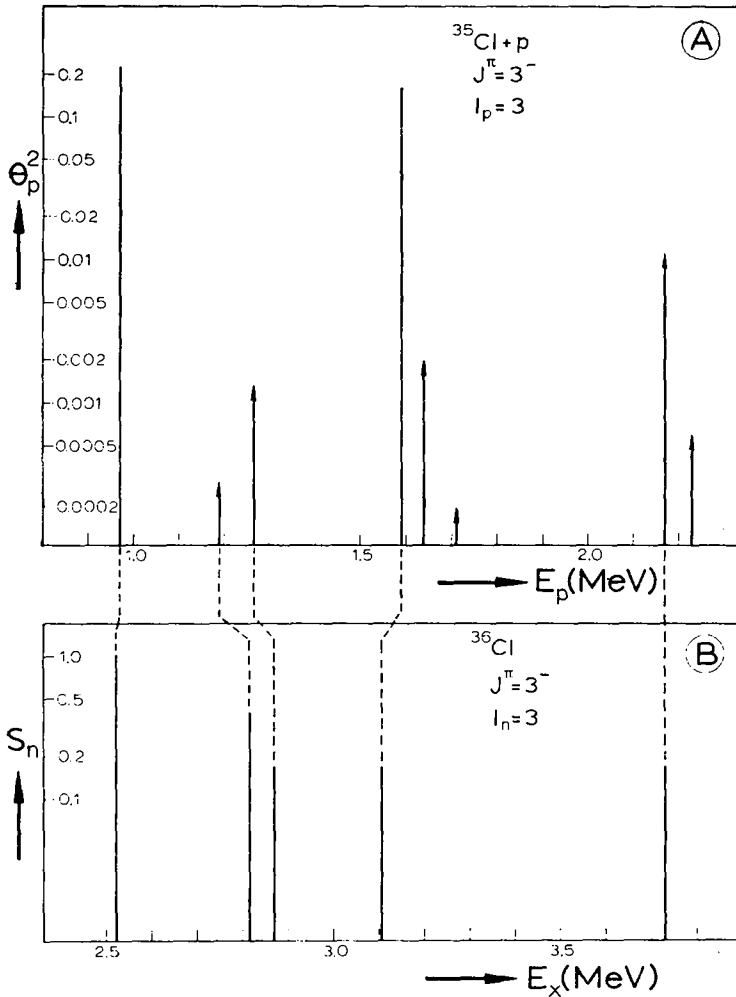


Fig. 9. Comparison of reduced proton widths $\theta_p^2(l_p = 3)$ in $^{35}\text{Cl} + p$ (A) and neutron spectroscopic factors $S_n(l_n = 3)$ in ^{36}Cl (B). Dashed lines connect analogue states in the ^{36}Ar - ^{36}Cl pair. The values are taken from tables 6 and 7 under the assumption that $J^\pi = 3^-$ for all states. Arrows indicate lower limits of θ_p^2 if Γ_{α_0}/Γ is unknown.

In the following, the analogue state assignments are discussed in more detail. The only known $^{35}\text{Cl} + p$ resonance between $E_p = 860$ and $1\,193$ keV with a measurable f-wave contribution is that at $E_p = 986$ keV with $J^\pi = 1^-, 2^+$ or 3^- . If this resonance is interpreted as the analogue of the $2\,522$ keV state in ^{36}Cl , the $J^\pi = 2^+$ as-

signment must be excluded. Of the two remaining assignments, the 3^- value is favoured, because the 1^- assignment would lead to a high value of $S_n = 2.3$.

The resonances in $^{35}\text{Cl}+p$ at $E_p = 1\,193$ keV ($J^\pi = 1^-, 3^-$) and $1\,264$ keV ($J^\pi = 1^-, 3^-, 4^+$) are interpreted as analogue states of the $E_x = 2\,816$ and $2\,868$ keV levels in ^{36}Cl .

Possible analogue states of the $E_x = 3\,103$ keV level in ^{36}Cl are the $E_p = 1\,518$ keV ($J^\pi = 1^-$), $1\,588$ keV ($J^\pi = 3^-$), $1\,637$ keV ($J^\pi = 1^-, 3^-$) and $1\,709$ keV ($J^\pi = 3^-$) resonances. The assumption of $J^\pi = 1^-$ for the $1\,637$ keV resonance is unlikely, because it would lead to 100 % f-capture at a strong resonance in competition with possible p-capture at rather low proton energy. Then the $1\,588$ keV resonance, possessing a measurable total width and is interpreted as the main analogue state component; the other $J^\pi = 3^-$ resonances appear possibly as weaker components of a split analogue state.

Possible analogous of the $E_x = 3\,728$ keV level in ^{36}Cl are the $E_p = 2\,172$ keV ($J^\pi = 3^-$) and the $2\,168$ keV ($J^\pi = 4^+, 5^-, 6^+$) resonances. The $2\,172$ keV resonance is the most likely candidate because of the extremely high $I_p = 3$ admixture amounting to 97 % (see table 3), and because of the larger reduced width. Table 7 contains the final conclusions on assignments of analogue resonances in $^{35}\text{Cl}+p$ to states in ^{36}Cl . The first two columns contain data on states in ^{36}Cl from the (d, p) work in ref. ¹⁹). Column 3 gives the reduced neutron widths S_n . Column 4 lists J^π values which follow from the present analogue state assignments. The next three columns contain data on the analogue resonances. The last column finally lists the Coulomb energy differences derived from the present assignments. In fig. 9, neutron spectroscopic factors of ^{36}Cl states and reduced proton widths of analogue resonances are plotted. The relative positions of the ^{36}Ar and ^{36}Cl energy scales are based on the average $\Delta E_C = 6\,960$ keV.

Theoretically, the relation $\theta_p^2 = \frac{1}{2}S_n$ should hold. Comparison of the measured θ_p^2 for $E_p = 968$ and $1\,588$ keV with the theoretical values shows an agreement within a factor of two. For the $E_p = 1\,193$, $1\,264$ and $2\,172$ keV resonances, where Γ_{α_0}/Γ is unknown, one finds from table 7 that the values of $\theta_p^2\Gamma_{\alpha_0}/\Gamma$ are much smaller than those of $\frac{1}{2}S_n$. The relatively small Γ_{α_0} values implied might be a reflection of the fact that for pure $T = 1$ states the (p, α_0) reaction is forbidden. It is hoped that (p, p) experiments on ^{35}Cl , being carried out at present in this laboratory, will yield more information on the partial proton widths.

The authors thank Professor P. M. Endt for his stimulating guidance and valuable suggestions. Dr. C. van der Leun kindly criticized the manuscript. The assistance of H. Berendsen and R. J. de Meijer during long runs is gratefully acknowledged.

This investigation was partly supported by the joint research program of the "Stichting voor Fundamenteel Onderzoek der Materie" and the "Nederlandse Organisatie voor Zuiver Wetenschappelijk Onderzoek".

References

- 1) F. C. Ern  and C. van der Leun, Nucl. Phys. **52** (1964) 515
- 2) F. C. Ern  and P. M. Endt, Nucl. Phys. **71** (1965) 593
- 3) F. C. Ern , Nucl. Phys. **84** (1966) 241
- 4) R. L. Clarke, E. Almqvist and E. B. Paul, Nucl. Phys. **14** (1959/60) 472
- 5) K. V. Karad ev, V. I. Man'ko and F. E.  ukreev, Yad. Fiz. **4** (1966) 909; Sov. J. Nucl. Phys. **4** (1967) 648
- 6) J. Kuperus, P. W. M. Glaudemans and P. M. Endt, Physica **29** (1963) 1281
- 7) B. Bo njakovi  and C. van der Leun, Phys. Lett. **23** (1966) 687
- 8) B. Bo njakovi , J. A. van Best and J. Bouwmeester, Nucl. Phys. **A94** (1967) 625
- 9) J. B. Marion, Revs. Mod. Phys. **38** (1966) 660
- 10) A. W. Borgi and O. L onsj , Internal Report, Fysisk Institutt, Universitetet i Oslo (1964)
- 11) J. H. E. Mattauch, W. Thiele and A. H. Wapstra, Nucl. Phys. **67** (1965) 32
- 12) H. A. van Rinsvelt and P. M. Endt, Physica **32** (1966) 513
- 13) P. M. Endt and C. van der Leun, Nucl. Phys. **A105** (1967) 1
- 14) L. Simons, E. Spring, A. Fontell, I. Forsblom, P. Holmberg and H. Jungner, Soc. Sci. Fennica, Comm. Phys.-Math. **30** (1965) 6
- 15) W. Bruynesteyn and B. Bo njakovi , Utrecht University (1967) unpublished
- 16) T. D. Newton, Can. J. Phys. **34** (1956) 804
- 17) A. Gilbert, F. S. Chen and A. G. W. Cameron, Can. J. Phys. **43** (1965) 1248
- 18) R. J. de Meijer and B. Bo njakovi , Utrecht University (1967) unpublished
- 19) A. M. Hoogenboom, E. Kashy and W. W. Buechner, Phys. Rev. **128** (1962) 305
- 20) G. van Middelkoop and P. Spilling, Nucl. Phys. **77** (1966) 267
- 21) J. Kopeck y, W. Raty nski and E. Warming, Ris  Report No. 157 (1967)
- 22) J. Rapaport and W. W. Buechner, Nucl. Phys. **83** (1966) 80
- 23) M. H. Macfarlane and J. B. French, Revs. Mod. Phys. **32** (1960) 567
- 24) R. E. Berg, J. L. Snelgrove and E. Kashy, Phys. Rev. **153** (1967) 1165